Effectiveness of Noise Reduction in LDCT Images Based on SRCNN

Doo Bin KIM[1], Hyun Mee PARK[2], Sang Hoon JOON[3], Joo Wan HONG[4]

Abstract

This study aims to evaluate the performance of noise reduction in LDCT images using an SRCNN based AI model. Using the Lungman phantom, images of effective mAs 72 recommended by AAPM and effective mAs 709 without using the AEC function were acquired. SRCNN model input image used a GT, label image and GT image was used as a low-resolution image. Image evaluation was conducted in the lung apex, middle level lung, and carina of trachea regions, and PSNR, SSIM, SSIM error map, SNR, MSE, and RMSE were used as evaluation indices are based on label image. Lung apex results showed increase of 19.52, 29.69 and 23.8%, and decreased of 71.37, 46.43% respectively. Middle level lung results showed increase of 20.99, 20.0 and 26.26%, and decreased of 72.67, 47.72% respectively. Carina of trachea results showed increase of 22.05, 32.31 and 28.18%, and decreased of 73.93, 48.93% respectively. Image evaluation results were improvement in image quality due to noise reduction was confirmed using the SRCNN based AI model. Therefore, confirmed that applying the SRCNN to LDCT images can improve image quality by reducing noise, and it is considered that AI based post processing will be useful for CT images without AI.

Keywords : LDCT, SRCNN, Noise, Denoising, PSNR

Major Classification Code: Artificial Intelligence

1. Introduction

Computed tomography (CT) uses X-ray to visualize the inside of the human body for internal medicine such as tumors of bleeding and surgical injuries caused by trauma. Because CT was possible to obtain anatomical radiography through a non-invasive, it is recognized as one of the essential radiography examinations for diagnosing various diseases. In addition, CT hardware and software have advanced compared to the past, resulting in relatively faster radiographic image acquisition times and improvements in radiographic image quality. However, despite technological advancements, radiographic image noise caused by X-ray and detector during CT scans results in a decrease in radiographic image quality (Diwakar et al., 2018). Noise in radiographic images can reduce the signal quality, significantly impacting the reading of medical radiographic images for diagnosing various diseases (Christianson, 2015). Due to this fundamental cause of noise, each CT manufacturer removes noise in various ways through software algorithms (Joemai, 2013; Fan, 2014; Ellmann, 2018). During a CT scan to examine lung tumors, nodules,

1 First Author. Professor, Department of Radiological Science, Cheju Halla University, Korea, Email: kdb095@chu.ac.kr
2 Second Author. M.D., Professor, Department of Radiology, National Medical Center, Korea, Email: dios1497@gmail.com
3 Third Author. Ph. D., Radiographer, Department of Radiology, National Medical Center, Korea, Email: rasist@mensakorea.org

4 Corresponding Author, Professor, Department of Radiological Science, Eulji University, Korea, Email: jwhong@eulji.ac.kr

or tuberculosis, high contrast was needed to clearly distinguish lung tissue, so a low dose Chest CT scan (Kubo et al., 2016, Asla et al., 2021). However, to improve contrast, using a low dose X-ray during CT scan increases noise, which in turn degrades image quality (Alshamari et al., 2015) Recently, artificial intelligence (AI) models that enhance low resolution to high resolution have been widely used in the entertainment industry, such as in movies and photography, showing improvements in image quality, including noise reduction and increased pixel count compared to the original. Latest CT equipped with iterative reconstruction algorithms or AI models were being introduced to improve image quality and reduce noise in radiographic imaging (Punwani et al., 2008, McLaughlin et al., 2014, Eisentopf et al., 2013). Therefore, this study aims to investigate the noise reduction performance when applying post processing to low dose chest CT images using a high resolution generating AI model based on Super Resolution Convolutional Neural Network (SRCNN).

2. Research Methods and Materials

2.1. Acquisition of CT Image Dataset

Lungman phantom (Chest Phantom N1, Kyoto Kagaku Inc., Japan) was used to acquire low dose chest CT images to be used for AI model learning. CT scans were performed using the Somatom Definition Force (Siemens Healthineers, Forchheim, Germany). Scan parameters were set according to the low dose screening CT protocol provided by AAPM: 100 kVp, pitch 1.2, rotation time 0.5 sec, spiral scan mode, slice thickness 1.0 mm, increment 0.7 mm, and ADMIRE strength 3. To obtain data corresponding to low resolution, images were acquired with an effective mAs 72 (Ground Truth Image, GT image) as recommended by AAPM (Alexandria, 2019). For data corresponding to high resolution, images were acquired with an effective mAs 709 (Label Image) without using the AEC function. Table 1 shows the CT scan parameter for image dataset acquisition.

Table 1: CT scan parameter for images dataset acquisition

Parameter	GT	Label
kVp	100	
Pitch	1.2	
Rotation Time (sec)	0.5	
Slice Thickness (mm)	1.0	
Increment (mm)	0.7	
Scan Mode	Spiral	
Admire Strength	3	
Effective mAs	72	709

Note: GT was Ground Truth, Effective mAs was mean mAs per unit length along the longitudinal axis (Effective mAs $= \frac{mAs}{Picth}$)

2.2. SRCNN Model Architecture

CT images were valuable for disease diagnosis, but data volume generated in a single scan was extremely large. To secure storage capacity on hard drives and other storage devices, 512 pixels were typically used as the standard. However, this can lead to difficulties in precise diagnosis. SRCNN model used in this study is less computer resource intensive compared to models such as enhanced deep super resolution network (EDSR), very deep convolutional networks (VDSR), and Generative Adversarial Network (GAN), making it a model that is not significantly affected by hardware limitations. Interpreter used for configuring the SRCNN model was Python (ver. 3.9.18). AI framework was TensorFlow (ver. 2.15.0) and Keras (ver. 2.15.0). For data preprocessing and visualization libraries were NumPy (ver. 1.26.2), pandas (ver. 2.1.4), OpenCV (ver. 4.10.0), and Matplotlib (ver. 3.8.2) were used. SRCNN model structure for denoising consists of a convolutional neural network (CNN) with three layers: patch extraction and representation ($F_1(Y)$) using 128 filters and kernel, non-linear mapping ($F_2(Y)$) using 64 filters and kernel, and reconstruction ($F(Y)$) using 3 filters and kernel (Chao Dong. Et al., 2015). Figure 1 shows the SRCNN architecture for low dose chest CT denoising.
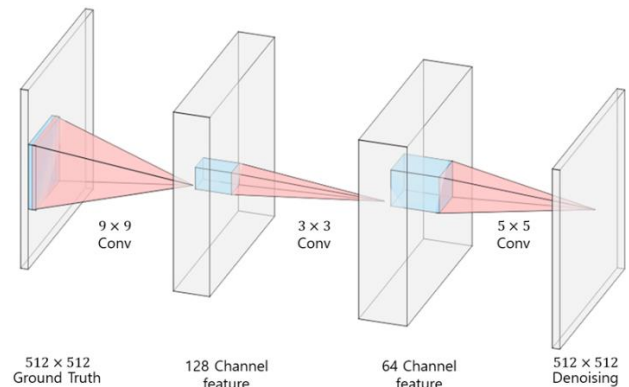

Figure 1: SRCNN architecture for low dose chest CT denoising

The equation for each layer was shown in Equation (1).

$$\begin{cases} F_1(Y) = \max(0, W_1 \times Y + B_1) \\ F_2(Y) = \max(0, W_2 \times F_1(Y) + B_2) \\ F(Y) = W_3 \times F_2(Y) + B_3 \end{cases} \quad (1)$$

where $F_1(Y)$ was patch extraction and representation, $F_2(Y)$ was Non-linear mapping, $F(Y)$ was Reconstruction or high resolution image, W was weight, Y was low resolution image, B was bias.

Input images used for model training utilized the GT images instead of converting the label images to low resolution. Prior to training, fixed parameters were set as follows: fix seed for reproducibility, epochs set to 50 to prevent overfitting, batch size set to 1 for observe consistent learning performance, learning rate was set default 0.0001 optimizer was set Adam, and padding set to same to maintain pixel dimensions. During model training, the optimizer used was Adam, the loss function was mean squared error (MSE), and the metrics used were peak signal to noise ratio (PSNR), structural similarity index map (SSIM).

2.3. Evaluation Indices of Image Noise

Evaluation of image noise was conducted by categorizing into three regions: lung apex where tuberculosis primarily occurs, middle level lung where neoplasms such as tumors occurs, and carina of the trachea where carcinoma of the lymph node occurs. Additionally, the analysis was performed using ImageJ software (National Institutes of Health, Bethesda, Maryland, ver. bundled with Java 8) based on the label images. The metrics used for noise evaluation included PSNR, SSIM, SSIM error map, signal to noise ratio (SNR), MSE, and root mean squared error (RMSE). All indices were mainly used when measuring noise in an image, and PSNR evaluates the loss information on image quality, and the unit is decibel (dB), and the lower the loss information in the image, the higher the value. The equation for PSNR was shown in Equation (2).

$$PSNR = 10\log\frac{S^2}{MSE} \tag{2}$$

where S was maximum value in images, MSE was mean squared error.

SSIM compares the luminance, contrast, and structure of two images to calculate the difference in image quality and similarity perceived by the visual organ, and indicates a higher value when the image information loss is less. The equation for SSIM was shown in Equation (3).

$$SSIM = \frac{(2\mu_x\mu_y+C_1)(2\sigma_{xy}+C_2)}{(\mu_x^2+\mu_y^2+C_1)(\sigma_x^2+\sigma_y^2+C_2)} \tag{3}$$

where x and y were comparison images, μ_x and μ_y were local means for images x and y, σ_x and σ_y were cross covariance for images x, y, C_1, C_2, and C_3 were dynamic range.

SNR was signal quality evaluation, and the higher the value, the less noise there is and the clearer the signal. The

equation for SNR was shown in Equation (4).

$$SNR = \frac{P_{signal}}{P_{noise}} \tag{4}$$

where P_{signal} was signal intensity, P_{noise} was signal noise.

MSE was quality measurement metric for image comparison, and it index a value close to 0 when the image is similar to the original. The equation for MSE was shown in Equation (5).

$$MSE = \frac{1}{n}\sum_{i=1}^n(\hat{Y}_i - Y_i)^2 \tag{5}$$

where n was number of datasets, $\hat{Y}_i$ was actual value, Y_i was predicted value.

RMSE was used to complement the drawback of increased error values due to squaring in MSE calculations, and it index a value close to 0 when the image was similar to the original. The equation for RMSE was shown in Equation (6).

$$RMSE = \sqrt{\frac{1}{n}\sum_{i=1}^n(\hat{Y}_i - Y_i)^2} \tag{6}$$

where n was number of datasets, $\hat{Y}_i$ was actual value, Y_i was predicted value.

3. Results

3.1. Results of SRCNN Model Training

During the training of the SRCNN model using a low-dose chest CT image dataset, it was confirmed that as the number of epochs increased, the loss decreased, and both PSNR and SSIM increased, indicating proper training. All metrics saturated at 50 epochs. Figure 2 shows the SRCNN model training graph based on loss, PSNR, SSIM metrics.
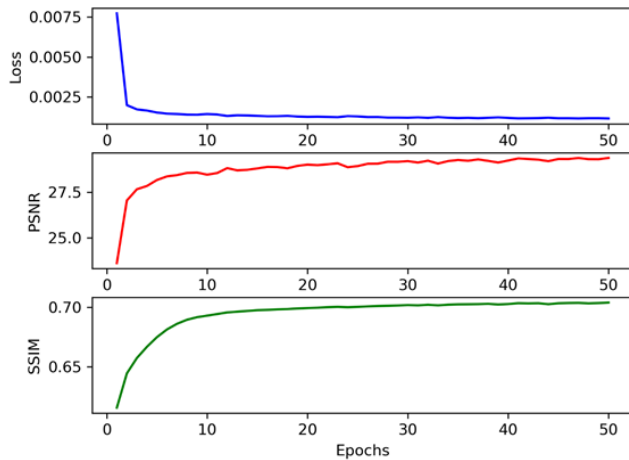
Figure 2: Results of SRCNN model training graph based on loss, PSNR, SSIM

Comparison three region images for each region using the model. Figure 3 shows the comparison of three region images.
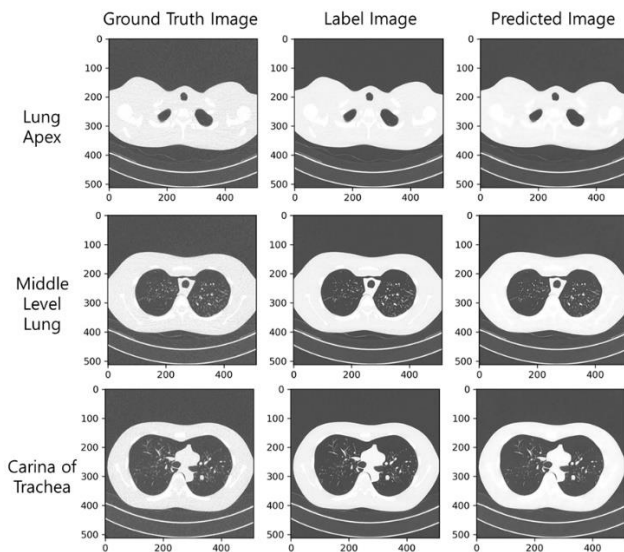

Figure 3: Results of images comparison by lung apex, middle level lung, carina of trachea

3.2. Results of Images Noise

Based on the label image, the PSNR of lung apex region image increased by 19.52% from GT and predicted images to 27.82 and 33.2 dB, respectively. SSIM increased by 29.69% to 0.64 and 0.83. SNR increased by 23.8% to 22.94 and 28.4. MSE decreased by 71.37% to 107.42 and 30.75. RMSE decreased by 46.43% to 10.36 and 5.55. For middle level lung region image, PSNR increased by 20.99% from GT and

predicted images to 26.82 and 32.45 dB, respectively. SSIM increased by 20.0% to 0.7 and 0.84. SNR increased by 26.26% to 21.48 and 27.12. MSE decreased by 72.67% to 135.36 and 36.99. RMSE decreased by 47.72% to 11.63 and 6.08. For carina of trachea region image, PSNR increased by 22.05% from GT and predicted images to 26.48 and 32.32 dB, respectively. SSIM increased by 32.31% to 0.65 and 0.86. SNR increased by 28.18% to 20.3 and 26.7. MSE decreased by 73.93% to 146.35 and 38.15. RMSE decreased by 48.93% to 12.1 and 6.18. Table 2 shows the images evaluation indices.

Table 2: Results of images evaluation indices

Index	Region					
	Apex		Mid.		Carina	
	GT	Pred.	GT	Pred.	GT	Pred.
PSNR	27.82	33.25	26.82	32.45	26.48	32.32
SSIM	0.64	0.83	0.70	0.84	0.65	0.86
SNR	22.94	28.40	24.48	27.12	20.83	26.70
MSE	107.42	30.75	135.36	36.99	146.35	38.15
RMSE	10.36	5.55	11.63	6.08	12.10	6.18

Note: GT was Ground Truth Image, Pred. was Predicted image on SRCNN, Mid. was middle.

Evaluation of image noise in low dose chest CT revealed that the signal and image similarity increased in all regions, while noise decreased. This was further confirmed through the SSIM error map, which demonstrated noise reduction and increased image similarity. Figure 4 shows the comparison of three region images of SSIM map.
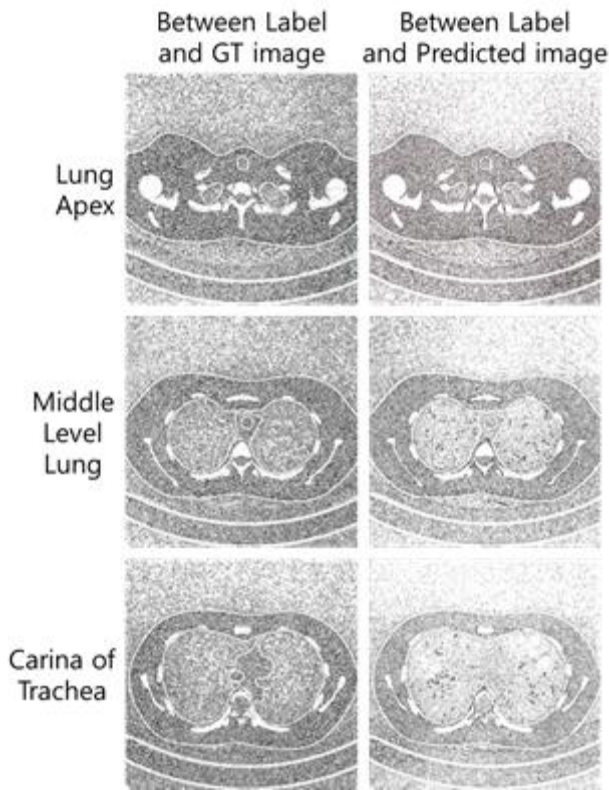
Figure 4: Comparison of SSIM map results between GT and Predicted image based on Label image

4. Discussion

CT scans use X-rays to non-invasively visualize the anatomical structure of internal organs, providing crucial medical radiographic images for diagnosing medical and surgical conditions. However, this method also has the downside of exposing patients to radiation. Despite of CT scans are applied because the goal of maintaining life is clear. Consequently, several CT manufacturers have been working hard to reduce radiation doses and achieve optimal imaging. Still, noise caused by the limitations of X-rays and mechanical factors cannot be entirely eliminated (Diwakar, M., 2018, McLaughlin, P. D., 2014, Li, Z., 2014). Therefore, this study aimed to confirm that AI models were useful for noise reduction. Original SRCNN model generates a low resolution image and performs end to end mapping with the corresponding high resolution image using a simple CNN structure (Dong et al., 2015). Since its release in 2015, various noise reduction models using CNN, GAN, and transformer models have been developed (Sadia et al. 2024). In previous studies on CNN based denoising models, Yufei Tang et al. found that the content-noise complementary network with contrastive learning (CCN-CL) model

increased PSNR and SSIM by 12.8 and 5.6%, respectively, and reduced RMSE by 37.6% (Tang, 2022). Additionally, Li et al. previous studies on the multistage convolutional neural networks (MSCNN) model increased PSNR and SSIM by 28.9 and 15.5%, respectively, demonstrating noise reduction (Li, 2022). Among previous studies on GAN based denoising models, Fu, Bo et al. found that the NGRNet model resulted in a PSNR increase 0.13 dB (Fu, 2022). All AI models for low dose CT noise reduction showed good results, but some models showed an increase in computational load as the number of model layers increased. In this study, SRCNN based on model showed satisfactory denoising results with simple layers and low computational load. However, compared to previous studies, the SSIM was relatively lower, which is likely due to the insufficient computational capacity of the shallow layers. Therefore, further research with increased layers is necessary. Additionally, the images generated by the SRCNN model are visually similar to the label images, suggesting that if the AI model is applied with a reduced dose during CT scans, patient radiation exposure could also be reduced.

5. Conclusions

In this study confirmed that the application of the SRCNN model to low-dose chest CT images can improve image quality by reducing noise. AI based post processing could also be beneficial for CT images without AI application.

References

Alshamari, M., Geijer, M., Norrman, E., Lidén, M., Krauss, W., Wilamowski, F., & Geijer, H. (2016). Low dose CT of the lumbar spine compared with radiography: a study on image quality with implications for clinical practice. *Acta Radiologica*, *57*(5), 602-611. https://doi.org/10.1177/0284185115595667

American Association of Physicists in Medicine. (2019). Lung Cancer Screening CT Protocols, Version 5.1. Alexandria, VA.

Aslan, S., Bekci, T., Çakır, İ. M., Ekiz, M., Yavuz, I., & Şahin, A. M. (2021). Diagnostic performance of low-dose chest CT to detect COVID-19: A Turkish population study. *Diagnostic and Interventional Radiology*, *27*(2), 181. https://doi.org/10.5152/dir.2020.20350

Christianson, O., Winslow, J., Frush, D. P., & Samei, E. (2015). Automated technique to measure noise in clinical CT examinations. *American Journal of Roentgenology*, *205*(1), W93-W99. https://doi.org/10.2214/AJR.14.13613

Diwakar, M., & Kumar, M. (2018). A review on CT image noise and its denoising. *Biomedical Signal Processing and Control*, *42*, 73-88. https://doi.org/10.1016/j.bspc.2018.01.010

Dong, C., Loy, C. C., He, K., & Tang, X. (2015). Image super-

resolution using deep convolutional networks. *Preprint* on arXiv. https://doi.org/10.48550/arXiv.1501.00092

Eisentopf, J., Achenbach, S., Ulzheimer, S., Layritz, C., Wuest, W., May, M., ... & Pflederer, T. (2013). Low-dose dual-source CT angiography with iterative reconstruction for coronary artery stent evaluation. JACC: *Cardiovascular Imaging*, *6*(4), 458-465. https://doi.org/10.1016/j.jcmg.2012.10.023

Ellmann, S., Kammerer, F., Allmendinger, T., Hammon, M., Janka, R., Lell, M., ... & Kramer, M. (2018). Advanced modeled iterative reconstruction (ADMIRE) facilitates radiation dose reduction in abdominal CT. *Academic Radiology*, *25*(10), 1277-1284. https://doi.org/10.1016/j.acra.2018.01.014

Fan, J., Yue, M., & Melnyk, R. (2014). Benefits of ASiR-V reconstruction for reducing patient radiation dose and preserving diagnostic quality in CT exams. *White paper*, GE Healthcare.

Fu, B., Zhang, X., Wang, L., Ren, Y., & Thanh, D. N. (2022). A blind medical image denoising method with noise generation network. *Journal of X-Ray Science and Technology*, *30*(3), 531-547. https://doi.org/10.3233/XST-211098

Joemai, R. M., Veldkamp, W. J., Kroft, L. J., Hernandez-Giron, I., & Geleijns, J. (2013). Adaptive iterative dose reduction 3D versus filtered back projection in CT: evaluation of image quality. *American Journal of Roentgenology*, *201*(6), 1291-1297. https://doi.org/10.2214/AJR.12.9780

Kubo, T., Ohno, Y., Nishino, M., Lin, P. J., Gautam, S., Kauczor, H. U., & iLEAD Study Group. (2016). Low dose chest CT protocol (50ámAs) as a routine protocol for comprehensive assessment of intrathoracic abnormality. *European Journal of Radiology Open*, *3*, 86-94. https://doi.org/10.1016/j.ejro.2016.04.001

Li, Q., Li, S., Li, R., Wu, W., Dong, Y., Zhao, J., ... & Aftab, R. (2022). Low-dose computed tomography image reconstruction via a multistage convolutional neural network with autoencoder perceptual loss network. *Quantitative Imaging in Medicine and Surgery*, *12*(3), 1929. https://doi.org/10.21037/qims-21-465

Li, Z., Yu, L., Trzasko, J. D., Lake, D. S., Blezek, D. J., Fletcher, J. G., ... & Manduca, A. (2014). Adaptive nonlocal means filtering based on local noise level for CT denoising. *Medical physics*, *41*(1), 011908. https://doi.org/10.1118/1.4851635

McLaughlin, P. D., Murphy, K. P., Hayes, S. A., Carey, K., Sammon, J., Crush, L., ... & Maher, M. M. (2014). Non-contrast CT at comparable dose to an abdominal radiograph in patients with acute renal colic; impact of iterative reconstruction on image quality and diagnostic performance. *Insights into imaging*, *5*, 217-230. https://doi.org/10.1007/s13244-014-0310-z

Punwani, S., Zhang, J., Davies, W., Greenhalgh, R., & Humphries, P. (2008). Paediatric CT: the effects of increasing image noise on pulmonary nodule detection. *Pediatric radiology*, *38*, 192-201. https://doi.org/10.1007/s00247-007-0694-8

Sadia, R. T., Chen, J., & Zhang, J. (2024). CT image denoising methods for image quality improvement and radiation dose reduction. *Journal of Applied Clinical Medical Physics*, *25*(2), e14270. https://doi.org/10.1002/acm2.14270

Tang, Y., Du, Q., Wang, J., Wu, Z., Li, Y., Li, M., ... & Zheng, J. (2022). CCN-CL: A content-noise complementary network with contrastive learning for low-dose computed tomography denoising. *Computers in Biology and Medicine*, *147*, 105759. https://doi.org/10.1016/j.compbiomed.2022.105759